

CERN-PH-EP-2013-163
24 August 2013

J/ψ production and nuclear effects in p-Pb collisions at $\sqrt{s_{NN}}=5.02$ TeV

ALICE Collaboration*

Abstract

Inclusive J/ψ production has been studied with the ALICE detector in p-Pb collisions at the nucleon–nucleon center of mass energy $\sqrt{s_{NN}} = 5.02$ TeV at the CERN LHC. The measurement is performed in the center of mass rapidity domains $2.03 < y_{\text{cms}} < 3.53$ and $-4.46 < y_{\text{cms}} < -2.96$, down to zero transverse momentum, studying the $\mu^+\mu^-$ decay mode. In this paper, the J/ψ production cross section and the nuclear modification factor R_{pPb} for the rapidities under study are presented. While at forward rapidity, corresponding to the proton direction, a suppression of the J/ψ yield with respect to binary-scaled pp collisions is observed, in the backward region no suppression is present. The ratio of the forward and backward yields is also measured differentially in rapidity and transverse momentum. Theoretical predictions based on nuclear shadowing, as well as on models including, in addition, a contribution from partonic energy loss, are in fair agreement with the experimental results.

arXiv:1308.6726v3 [nucl-ex] 20 Nov 2014

*See Appendix A for the list of collaboration members

The production of charmonia, bound states of c and \bar{c} quarks, is the object of intense theoretical and experimental investigations [1]. As of today, their production mechanism in pp collisions is described by models based on Quantum Chromodynamics (QCD). In particular, in the NRQCD (non-relativistic QCD) approach [2], charmonium production is seen as a two-step process which includes the creation of the $c\bar{c}$ pair in a hard scattering, described perturbatively, and the subsequent evolution of the pair towards a bound state with specific quantum numbers, which is modeled in a non-perturbative way. In this model, the evolving $c\bar{c}$ pair can be in a color-singlet (CS) as well as in a color-octet (CO) state, with the strength of the CO amplitude contributions being controlled by non-perturbative factors, extracted by fits to experimental data (see [3] for a recent implementation based on HERA, RHIC and LHC results).

Several initial/final-state effects related to the presence of cold nuclear matter can influence the observed charmonium yields in proton-nucleus collisions. Concerning the initial state, the kinematical distributions of partons in nuclei are different from those in free protons and neutrons (nuclear shadowing [4–8]), affecting the production cross section of the $c\bar{c}$ pair. Therefore, charmonium production measurements help in constraining the nuclear parton distribution functions for gluons, which at hadron collider energies dominate the production process. Alternatively, when the production process is dominated by low-momentum gluons, i.e. carrying a small fraction x_{Bj} (Bjorken- x) of the momentum of the hadron, the Color-Glass Condensate (CGC) effective theory [9, 10] describes the nucleus as a dense (saturated) partonic system, and gives, once it is combined with a specific pp production model, predictions for the charmonium yields. In addition, the initial parton inside the proton may suffer energy loss before the hard collision producing the $c\bar{c}$ pair takes place, shifting in this way the center-of-mass energy \sqrt{s} of the partonic collision [11–13]. This effect can result in a suppression of charmonia at large longitudinal momentum.

Once created, the evolving $c\bar{c}$ pair needs a finite amount of time (up to several fm/ c in the nucleus rest frame) to form the final-state charmonium. It may, therefore, interact with the nuclear matter and possibly break-up, with the break-up cross section being sensitive to the nature (color-octet or singlet) of the intermediate state [14–16]. In addition, the final state may also experience energy loss, leading to a reduction of the pair momentum [17]. It is also worth noting that recent approaches to the parton energy loss effect led to the hypothesis of a coherent energy loss which cannot be factorized into initial and final-state contributions [13].

Experimental studies have been carried out at various collision energies, for nuclei of different sizes, and differentially in rapidity (y) and transverse momentum (p_{T}). These studies allow the amount of nuclear matter crossed by the $c\bar{c}$ pair to be varied, modifying the environment of its evolution, as well as the initial parton kinematics. In this way, further constraints to theoretical models can be provided.

Finally, the small size (< 1 fm) and large binding energy (several hundred MeV) of some of the charmonium states make them ideal probes of the strongly interacting matter created in ultrarelativistic heavy-ion collisions, which at sufficiently high energy density may become a Quark-Gluon Plasma (QGP). A suppression of charmonium production was predicted as a signature of the phase transition to a QGP [18] and observed at SPS [19–21] ($\sqrt{s_{\text{NN}}} \sim 20$ GeV) and RHIC [22, 23] ($\sqrt{s_{\text{NN}}} = 200$ GeV), and more recently at the LHC [24–27] ($\sqrt{s_{\text{NN}}} = 2.76$ TeV). However, in such collisions, suppression mechanisms related to initial-state effects and/or interaction of charmonia with cold nuclear matter have been verified to play a role [28, 29]. Results on proton-nucleus collisions are therefore essential to calibrate and disentangle these effects in order to allow a quantitative determination of the QGP-related suppression in nucleus-nucleus collisions.

A large amount of experimental results is available today for the production of J/ ψ , the most strongly bound charmonium state decaying into dileptons, in proton-nucleus collisions. Fixed-target experiments at SPS [30, 31], Tevatron [32] and HERA [33], as well as collider experiments at RHIC [34] have investigated J/ ψ production in large kinematic ranges in the Feynman- x ($x_{\text{F}} = 2p_{\text{L}}/\sqrt{s}$, where p_{L} is the

longitudinal momentum) and p_{T} variables. Among the main features of the results, a suppression of the J/ψ yield, relative to the one in proton-proton collisions, has been observed, which increases at high x_{F} (corresponding to forward y). In addition, at fixed x_{F} the suppression decreases with increasing $\sqrt{s_{\text{NN}}}$ [31]. Finally, the suppression is found to steadily decrease [32, 33] as a function of p_{T} . Several attempts have been made to describe these observations theoretically, based on the different physics mechanisms described above [17]. Although some features of the data are correctly reproduced, a quantitative understanding has not yet been reached.

In this context, data from the LHC can bring new information and help to clarify the situation. On the production side, very small x_{Bj} values, down to $\sim 10^{-5}$, can be accessed, allowing the gluon distributions to be studied in a previously unexplored kinematic range. On the other hand, the large Lorentz γ -factor of the $c\bar{c}$ pair, in particular at forward y , makes its crossing time through nuclear matter very short. In this kinematic range one may therefore expect a negligible $c\bar{c}$ break-up probability and the yield to be dominated by initial-state effects and possibly energy loss. In addition, proton-nucleus results are essential, as it was the case at lower energies [19], in the interpretation of the J/ψ suppression effects seen in Pb-Pb collisions at the LHC.

In this paper, we present the first results from ALICE on inclusive J/ψ production at the LHC in p-Pb collisions at $\sqrt{s_{\text{NN}}} = 5.02$ TeV. These results have been obtained with measurements in the $\mu^+\mu^-$ decay channel in the muon spectrometer, which covers the pseudorapidity range $-4 < \eta_{\text{lab}} < -2.5$. The muon spectrometer [35] consists of a 3 T-m dipole magnet, five tracking stations, each one based on two Cathode Pad Chambers, and two triggering stations, each one equipped with two planes of Resistive Plate Chambers. Two absorbers efficiently filter out hadrons. The front absorber, which is placed between the interaction region and the muon spectrometer, has a thickness of 10 interaction lengths (λ_{I}), while a second absorber, placed between the tracking and the triggering stations, has a thickness of 7.2 λ_{I} . The other detectors used in this analysis are the two Si pixel layers corresponding to the innermost sections of the Inner Tracking System (ITS) ($|\eta_{\text{lab}}| < 0.9$) [36], for the determination of the interaction vertex, and the two VZERO scintillator hodoscopes ($2.8 < \eta_{\text{lab}} < 5.1$ and $-3.7 < \eta_{\text{lab}} < -1.7$) [37], mainly for triggering purposes and for removing beam-induced background. The Zero Degree Calorimeters (ZDC) [38], positioned symmetrically at 112.5 m from the interaction point, are used to clean the event sample by removing de-bunched proton-lead collisions. More details on the ALICE experimental setup can be found elsewhere [39].

Minimum-bias (MB) events are triggered requiring the coincidence of a signal in the two VZERO detectors. The efficiency of such a trigger for selecting non single-diffractive collisions is $> 99\%$ [40]. A simulation based on Monte-Carlo (MC) event generators has shown that the contamination from single-diffractive and electromagnetic interactions is negligible [40]. Opposite-sign muon pairs are selected by means of a dimuon trigger given by the coincidence of a MB trigger with the detection of two muon candidate tracks in the trigger system of the muon spectrometer. The dimuon trigger is configured in order to select muons having a transverse momentum $p_{\text{T},\mu} > 0.5$ GeV/c. The effect of this threshold is not sharp and the single-muon trigger efficiency reaches its plateau value ($\sim 96\%$) for $p_{\text{T},\mu} \sim 1.5$ GeV/c. Events with more than a single interaction per bunch crossing (pile-up events) represent $\sim 2\%$ of MB triggered events, while the probability of having two dimuon triggers in the same bunch crossing is negligible.

Due to the energy asymmetry of the LHC beams ($E_{\text{p}} = 4$ TeV, $E_{\text{Pb}} = 1.58 \cdot A_{\text{Pb}}$ TeV, where $A_{\text{Pb}}=208$ is the Pb-nucleus mass number) the nucleon-nucleon center-of-mass system of the collisions does not coincide with the laboratory system, but is shifted by $\Delta y = 0.465$ in the direction of the proton beam. Data have been taken with two beam configurations, by inverting the sense of the orbits of the two particle species. In this way the regions $2.03 < y_{\text{cms}} < 3.53$ and $-4.46 < y_{\text{cms}} < -2.96$ have been studied, where positive rapidities refer to the situation where the proton beam is travelling towards the muon spectrometer (in the following these configurations are referred to as p-Pb and Pb-p, respectively). The integrated luminosities used in this analysis for the two configurations are 5.01 ± 0.17 nb $^{-1}$ (p-Pb) and 5.81 ± 0.18 nb $^{-1}$ (Pb-p).

These values are determined using $\sigma_{pPb}^{MB} = 2.09 \pm 0.06$ b and $\sigma_{PbPb}^{MB} = 2.12 \pm 0.06$ b, estimated by means of van-der-Meer scans of the MB trigger signal [41].

An offline selection is performed in order to reject beam-induced background by requiring the signal timing in the VZERO and ZDC to be compatible with that of a nominal p-Pb interaction. Candidate muon tracks are reconstructed in the muon tracking chambers using the standard reconstruction algorithm [35]. It is then required that the two reconstructed tracks match a track segment in the trigger chambers (trigger tracklet). A further selection cut is applied by requiring the muon tracks to exit the front absorber at a radial distance from the beam axis $17.6 < R_{abs} < 89.5$ cm, in order to reject tracks crossing its high-density section, where multiple scattering and energy loss effects are large. The condition $-4 < \eta_{lab,\mu} < -2.5$ for single muons is required, in order to reject muons at the edge of the spectrometer's acceptance. No cut on the z -position of the interaction vertex is carried out, since it was verified that the dimuon invariant mass resolution does not depend on it.

The extraction of the number of J/ψ is performed starting from the invariant mass distributions of opposite sign muon pairs in the kinematic domain $2.5 < |y_{lab}| < 4$, $p_T < 15$ GeV/c, shown in Fig. 1. The distributions are fitted by means of a superposition of a continuum and a resonance shape. The continuum is parameterized either as a polynomial times an exponential function or as a Gaussian with a width linearly varying with mass, while for the resonance either a Crystal Ball function [42] with asymmetric tails at both high and low mass was chosen, or various pseudo-Gaussian functions (see, for example, [43]). The non-Gaussian tails of the resonance shapes are fixed in the fit to the values obtained in a MC simulation of the J/ψ signal, while the mean and the width of the Gaussian core are left as free parameters, since the large signal-over-background ratio (~ 2 at $3\text{-}\sigma$ level) allows the data themselves to better constrain these parameters. The widths extracted from data (~ 70 MeV/c²) are larger by $\sim 10\%$ than those from MC, and the mean value of the J/ψ mass coincides with the nominal PDG value [44] within $\sim 0.1\%$. The $\psi(2S) \rightarrow \mu^+\mu^-$ decay is taken into account in the fit function, but its effect on the determination of the number of J/ψ events is negligible. The latter number is obtained as an average of the integral of the signal function over the various fits, and the systematic uncertainty on this quantity is taken as the $1\text{-}\sigma$ spread of the number of signal events. The result is $N_{pPb}^{J/\psi} = (6.69 \pm 0.05 \pm 0.08) \cdot 10^4$ and $N_{PbPb}^{J/\psi} = (5.67 \pm 0.05 \pm 0.07) \cdot 10^4$, where the first uncertainty is statistical and the second is systematic.

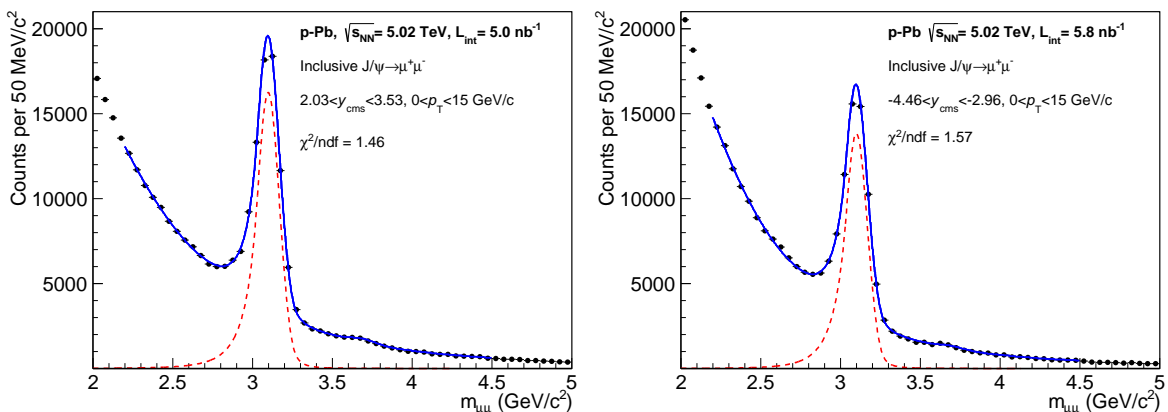


Fig. 1: The opposite-sign dimuon invariant mass spectra for the p-Pb (left) and Pb-p (right) data samples, together with the result of the fit. For the fits shown here a Crystal Ball function (shown as a dashed line) and a variable-width Gaussian have been used for the signal and the background, respectively.

The number of measured J/ψ is then divided by the product of acceptance times efficiency $A \cdot \epsilon$, which is obtained using a MC simulation of the J/ψ signal. An unpolarized distribution for the J/ψ is assumed, following the small degree of polarization measured in pp collisions at $\sqrt{s} = 7$ TeV [45–47], while the p_T and y distributions used as an input for the generator are tuned to the measured data through an iterative

procedure. The systematic uncertainty on the acceptance is obtained by defining y (p_T) distributions for selected phase space regions, corresponding to sub-ranges in p_T (y) and centrality of the collision. The hardest and softest spectra for each variable are then used as inputs to the MC calculation, and the variation with respect to the default acceptance values gives the systematic uncertainty, which amounts to 1.5% for both p-Pb and Pb-p.

The efficiency of the muon triggering detectors is calculated with a procedure based on data and involving the analysis of trigger tracklets constructed from hits in the four planes of the two trigger stations. For the tracking chambers a map of dead channels is obtained from the online detector information and updated on a run-per-run basis. Both information are injected in the MC and their time evolution is taken into account by performing a simulation for each run, with a number of J/ψ signal events proportional to the number of offline-selected triggered events.

The systematic uncertainty on the J/ψ trigger efficiency ($\epsilon_{\text{trig}}^{J/\psi}$) is obtained as a convolution of various sources. First, effects related to the estimate of the efficiency of the trigger detectors are studied by varying their efficiency in the MC by an amount equal to the statistical uncertainty on their evaluation ($\sim 2\%$). This results in a 2% change in $\epsilon_{\text{trig}}^{J/\psi}$. Second, systematic effects related to small discrepancies in the p_T dependence of the muon trigger threshold between data and MC give a $\sim 2 - 2.5\%$ contribution to $\epsilon_{\text{trig}}^{J/\psi}$. Finally, there is a $\sim 1\%$ effect related to the choice of the goodness-of-fit χ^2 cut used in defining the matching between tracking and triggering information.

The single-muon tracking efficiencies are obtained using an algorithm based on reconstructed tracks [35]. The systematic uncertainty on this quantity is obtained by comparing the results obtained with MC and real data. This uncertainty is considered as fully uncorrelated between the two detected muons and, at the dimuon level, it amounts to 4% (6%) for p-Pb (Pb-p). In addition, it was checked that the tracking efficiency does not depend on the centrality of the collision, justifying the use of pure signal MC simulations to determine $A \cdot \epsilon$.

The average $A \cdot \epsilon$ values for the two kinematic regions are $(25.4 \pm 1.3)\%$ (p-Pb) and $(17.1 \pm 1.2)\%$ (Pb-p). The quoted uncertainty is systematic, and the lower value for Pb-p is mainly due to a smaller detector efficiency in the corresponding data taking period.

The inclusive J/ψ production cross section is

$$\sigma_{\text{pPb}}^{J/\psi} = \frac{N_{J/\psi \rightarrow \mu\mu}^{\text{cor}}}{N_{\text{MB}} \cdot \text{B.R.}(J/\psi \rightarrow \mu\mu)} \times \sigma_{\text{pPb}}^{\text{MB}} \quad (1)$$

where $N_{J/\psi \rightarrow \mu\mu}^{\text{cor}}$ is the number of J/ψ corrected for $A \cdot \epsilon$, $\text{B.R.}(J/\psi \rightarrow \mu\mu) = (5.93 \pm 0.06)\%$ is the branching ratio for the J/ψ decay to dimuons [44], N_{MB} is the number of MB p-Pb collisions, and $\sigma_{\text{pPb}}^{\text{MB}}$ the corresponding cross section.

Since the analysis is based on a dimuon trigger sample, the equivalent number of MB triggers is evaluated as $F \cdot N_{\text{DIMU}}$, where N_{DIMU} is the number of opposite sign dimuon triggered events, which amounts to $9.27 \cdot 10^6$ for p-Pb and $2.09 \cdot 10^7$ for Pb-p. The enhancement factor F is calculated in two different ways. In the first one it is obtained as the product $F_{2\mu/1\mu} \cdot F_{1\mu/\text{MB}}$, where $F_{2\mu/1\mu}$ is the inverse of the probability of having a second muon triggered when one muon has triggered the event and, correspondingly, $F_{1\mu/\text{MB}}$ is the inverse of the probability of having one triggered muon in events where the MB condition is required. The various quantities are obtained from the recorded trigger mask for the collected events after quality cuts. Obtaining F as the product of the two factors mentioned above allows the statistical uncertainty to be reduced. In the second approach, the information of the counters recording the number of level-0 triggers is used. In this case, statistics are much larger and F is obtained as the ratio between the numbers of MB and dimuon triggers at level-0, corrected for pile-up effects (2%) and taking into account

Table 1: Systematic uncertainties (in percent) contributing to the measurement of inclusive J/ψ cross sections and nuclear modification factors. When the uncertainty values depend on the rapidity bin under consideration, their maximum and minimum values are quoted. Uncertainties on σ_{pPb}^{MB} are relevant for inclusive J/ψ cross sections only, while those on $\sigma_{pp}^{J/\psi}$ and $\langle T_{pPb} \rangle$ contribute only to the uncertainty on the nuclear modification factors.

Source	$\sigma_{pPb}^{J/\psi}, R_{pPb}$	$\sigma_{Pbp}^{J/\psi}, R_{Pbp}$
<i>Uncorrelated</i>		
Tracking efficiency	4	6
Trigger efficiency	2.8	3.2
Signal extraction	1.3 (1.5 – 3.4)	1.2 (1.6 – 3.8)
MC input	1.5 (1.1 – 3)	1.5 (0.9 – 4.2)
Matching efficiency	1	1
F	1	1
$\sigma_{pp}^{J/\psi}$	4.3 (3.1 – 6.0)	4.6 (3.1 – 13.4)
<i>Partially correlated</i>		
σ_{pPb}^{MB}	3.2	3
$\sigma_{pp}^{J/\psi}$	3.7 (2.7 – 9.2)	3.1 (1.2 – 8.3)
<i>Correlated</i>		
B.R.		1
$\langle T_{pPb} \rangle$		3.6
$\sigma_{pp}^{J/\psi}$		5.5

the slight difference in the fraction of events surviving the quality cuts for the two trigger samples (1%). One gets, averaging the results from the two approaches, $F_{pPb} = 1129 \pm 2$ and $F_{Pbp} = 589 \pm 2$, where the quoted uncertainties are statistical. A 1% systematic uncertainty is estimated on both quantities, corresponding to the difference between the values obtained in the two calculations.

Finally, the quantity N_{MB}/σ_{pPb}^{MB} corresponds to the integrated luminosity. As a cross-check, its value has been measured independently by using a second reference trigger, issued by a Čerenkov counter [39], whose cross section was also measured in the van-der-Meer scans. The luminosities measured with the two luminometers differ by at most 1% throughout the whole data-taking period. This small difference (identical for p-Pb and Pb-p) has been included in the systematic uncertainty on σ_{pPb}^{MB} .

The resulting cross sections are

$$\begin{aligned} \sigma_{pPb}^{J/\psi}(2.03 < y_{cms} < 3.53) &= 886 \pm 6(\text{stat.}) \pm 48(\text{syst.uncorr.}) \pm 30(\text{syst.part.corr.}) \mu\text{b} \\ \sigma_{Pbp}^{J/\psi}(-4.46 < y_{cms} < -2.96) &= 966 \pm 8(\text{stat.}) \pm 70(\text{syst.uncorr.}) \pm 31(\text{syst.part.corr.}) \mu\text{b} \end{aligned}$$

The uncertainties connected with tracking, matching and triggering efficiency, with signal extraction, with the choice of the MC input distributions and with the evaluation of N_{MB} are taken as uncorrelated between p-Pb and Pb-p, while those on σ_{pPb}^{MB} are partially correlated. In the latter uncertainty a 1% contribution due to the uncertainty on B.R.(J/ψ → μμ) was also included. A summary of the sources of systematic uncertainties and their numerical values are given in Table 1.

The nuclear effects on J/ψ production are quantified using the nuclear modification factor R_{pPb} , obtained as

$$R_{pPb} = \frac{N_{J/\psi \rightarrow \mu\mu}^{\text{cor}}}{\langle T_{pPb} \rangle \cdot N_{MB} \cdot \text{B.R.}(J/\psi \rightarrow \mu\mu) \cdot \sigma_{pp}^{J/\psi}} \quad (2)$$

where $\sigma_{pp}^{J/\psi}$ is the production cross section in pp collisions in the same kinematical domain and at the same \sqrt{s} (the same formula applies to Pb-p), and $\langle T_{pPb} \rangle$ is the nuclear thickness function estimated

through the Glauber model, which gives $\langle T_{\text{pPb}} \rangle = 0.0983 \pm 0.0035 \text{ mb}^{-1}$ [48]. The uncertainty on $\langle T_{\text{pPb}} \rangle$ was obtained by varying the parameters of the Glauber model.

Since pp data at $\sqrt{s} = 5.02$ TeV are not available, the reference cross section $\sigma_{\text{pp}}^{J/\psi}$ has been obtained by means of an interpolation procedure [49], based on forward rapidity ($2.5 < y_{\text{cms}} < 4$) pp results at $\sqrt{s} = 2.76$ and 7 TeV from ALICE [50, 51]. The \sqrt{s} -interpolation is based on three empirical shapes (linear, power law, exponential) and is independently performed for each of the six rapidity bins corresponding to the $d\sigma/dy$ values measured at the two energies. The central values of the interpolation are given, for each rapidity bin, by the average of the three values obtained with the adopted shapes. Their uncertainties are the quadratic sum of a dominant term, related to the uncertainties on the points used for the interpolation, and of a term corresponding to the maximum spread between the results obtained with the various shapes. A small additional systematic uncertainty is obtained comparing the empirical shapes with those calculated with the leading order (LO) CEM [52] and FONLL [53] models. We recall that the CEM (Color Evaporation Model) assumes that a fixed fraction of $c\bar{c}$ pairs produced with an invariant mass $m < 2m_{\text{D}}$ ends up in producing charmonium states. Although it does not contain a dynamical description of the production process, it was shown to be phenomenologically successful over a large \sqrt{s} range. FONLL gives predictions for the total $c\bar{c}$ production rather than for the J/ψ cross section, but we assume, similarly to the CEM approach, that the fraction of $c\bar{c}$ pairs going to charmonium is \sqrt{s} -independent.

Due to the $\Delta y = 0.465$ rapidity shift induced by the asymmetry in the energy per nucleon of the proton and lead beams, the rapidity regions covered by the present analysis do not correspond to the ones available for pp. Therefore, the $d\sigma/dy$ values obtained at $\sqrt{s} = 5.02$ TeV with the procedure described above have been fitted to various shapes (Gaussian, second and fourth order polynomials [54]). The values for $\sigma_{\text{pp}}^{J/\psi}$ at $\sqrt{s} = 5.02$ TeV for the p-Pb and Pb-p rapidity intervals were finally obtained as the average of the integral of the various fitting functions in the corresponding y -ranges, and are $\text{B.R.} \cdot \sigma_{\text{pp}}^{J/\psi}(2.03 < y_{\text{cms}} < 3.53) = 367 \pm 29 \text{ nb}$ and $\text{B.R.} \cdot \sigma_{\text{pp}}^{J/\psi}(-4.46 < y_{\text{cms}} < -2.96) = 255 \pm 20 \text{ nb}$ [49]. The quoted total uncertainties include again a contribution from the maximum spread of the results obtained with the various functions.

The measured nuclear modification factors, shown in Fig. 2, are

$$R_{\text{pPb}}(2.03 < y_{\text{cms}} < 3.53) = 0.70 \pm 0.01(\text{stat.}) \pm 0.05(\text{syst.uncorr.}) \pm 0.03(\text{syst.part.corr.}) \pm 0.05(\text{syst.corr.})$$

$$R_{\text{PbP}}(-4.46 < y_{\text{cms}} < -2.96) = 1.08 \pm 0.01(\text{stat.}) \pm 0.09(\text{syst.uncorr.}) \pm 0.03(\text{syst.part.corr.}) \pm 0.07(\text{syst.corr.})$$

At forward rapidity the inclusive J/ψ production is suppressed with respect to the one in binary-scaled pp collisions, whereas it is unchanged at backward rapidity. The uncertainties related to $\langle T_{\text{pPb}} \rangle$ and $\text{B.R.}(J/\psi \rightarrow \mu\mu)$ are considered as correlated. The uncertainties connected with tracking, matching and triggering efficiencies, with signal extraction, with the choice of the MC input distributions, and with the evaluation of N_{MB} are taken as uncorrelated. Finally, the uncertainty on the pp cross section interpolation is splitted (see [49] for details) among the three uncertainties quoted for the nuclear modification factors. The numerical details on systematic uncertainties are given in Table 1. Our measurements are compared with a next to leading order (NLO) CEM calculation which uses the EPS09 shadowing parameterization [55], and with the result of a theoretical prediction which includes a contribution from coherent parton energy loss processes [56], either in addition to EPS09 shadowing or as the only nuclear effect. Finally, results from a calculation in the CGC framework [57], combined with a CEM production model, are also shown. Within our uncertainties, both the model based on shadowing only and the coherent energy loss approach are able to describe the data, while the CGC-based prediction overestimates the observed suppression. None of these models include a suppression related to the break-up of the $c\bar{c}$ pair.

It is worth noting that calculations refer to prompt production (i.e., direct J/ψ plus the contribution from $\psi(2\text{S})$ and χ_c decays), while the experimental results are for inclusive J/ψ production, which contains a

non-prompt contribution from B-decays. However, the p_T -integrated non-prompt J/ψ fraction is small (LHCb measured 7.1% at $\sqrt{s} = 2.76$ TeV in the kinematic region $2 < y_{cms} < 4.5$, $p_T < 12$ GeV/c [58] and 9.8% at $\sqrt{s} = 7$ TeV for $2 < y_{cms} < 4.5$, $p_T < 14$ GeV/c [59]). The difference between R_{pPb}^{incl} and R_{pPb}^{prompt} is well within the uncertainties of our measurement for a very large range of $R_{pPb}^{non-prompt}$, from almost complete suppression ($R_{pPb}^{non-prompt} = 0.2$) to a rather strong enhancement ($R_{pPb}^{non-prompt} = 1.3$). A similar conclusion holds at backward rapidity.

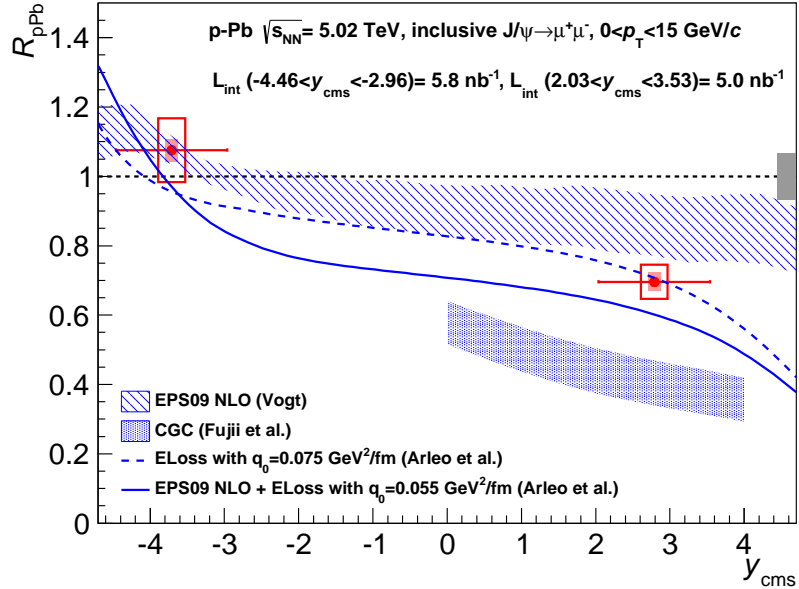


Fig. 2: The nuclear modification factors for inclusive J/ψ production at $\sqrt{s_{NN}} = 5.02$ TeV. The error bars correspond to the statistical uncertainties, the open boxes to the uncorrelated systematic uncertainties, the shaded boxes around the points represent the partially correlated systematic uncertainties. The box around $R_{pPb} = 1$ shows the size of the correlated uncertainties. Results from various models are also shown. The theoretical uncertainties for the EPS09 NLO calculation [55] are due to the uncertainty on the EPS09 shadowing parameterization and to the mass and scale uncertainties on the cross section calculation. For the CGC model [57], the band is related to the choice of the parton saturation scale and of the charm quark mass. Finally, the q_0 value in the energy loss model [56] represents the value of the transport coefficient in the target nucleons for $x_{Bj} = 10^{-2}$ gluons.

Both cross sections and nuclear modification factors for inclusive J/ψ have also been studied differentially in rapidity, with six bins for each of the two y domains. The results are shown in Fig. 3 and Fig. 4, respectively. The analysis procedure is identical to the one detailed above for the study of the integrated quantities. In particular, a differential estimate of the systematic uncertainties for the various ingredients has been carried out. The larger uncertainties visible at the lower edges of the rapidity ranges covered in p-Pb and Pb-p are related to a larger uncertainty on the pp reference cross section, due to the fact that these regions are not directly covered by the pp measurements and therefore an extrapolation has to be performed [49]. No strong variation of the nuclear modification factors is observed, in particular at backward rapidity, where models including coherent energy loss suggest a steeper behaviour.

Both $\sigma_{pp}^{J/\psi}$ and $\langle T_{pPb} \rangle$ cancel out when forming the ratio R_{FB} of the nuclear modification factors for a rapidity range symmetric with respect to $y_{cms} = 0$. In this way one is left with the ratio of the forward and backward J/ψ yields. The drawback of this approach is that, due to the beam energy asymmetry, the common y interval covered at both forward and backward rapidity is smaller than the acceptance of the muon spectrometer, and limited to $2.96 < |y_{cms}| < 3.53$. The reduction in statistics by a factor ~ 3 is compensated by the cancellation of the reference-related uncertainties. The obtained value is $R_{FB}(2.96 < |y_{cms}| < 3.53) = 0.60 \pm 0.01(\text{stat.}) \pm 0.06(\text{sys.})$. The systematic uncertainties which are uncorrelated

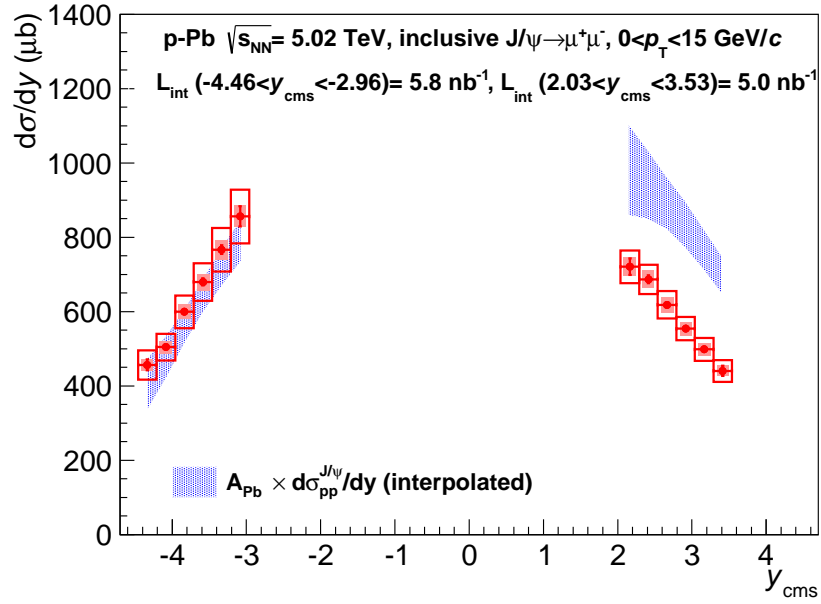


Fig. 3: The inclusive J/ψ production cross section, as a function of rapidity. The error bars correspond to the statistical uncertainties, the open boxes to the uncorrelated systematic uncertainties, the shaded boxes around the points represent the partially correlated systematic uncertainties. The bands correspond to the inclusive J/ψ pp cross section, obtained with the interpolation procedure described in the text and scaled by the Pb-nucleus mass number A_{Pb} .

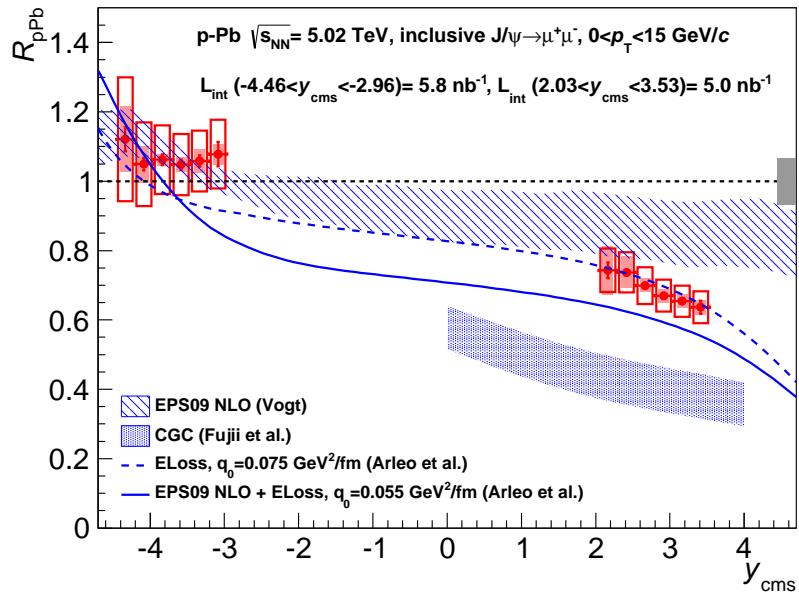


Fig. 4: The nuclear modification factors for inclusive J/ψ production at $\sqrt{s_{NN}} = 5.02$ TeV, in bins of rapidity. The meaning of symbols and curves is the same as in Fig. 2.

between backward and forward rapidity (tracking, matching and triggering efficiency, normalization, MC input) have been quadratically combined in the ratio, while for signal extraction the uncertainty has directly been calculated on the ratio of the number of J/ψ . The main contribution to the R_{FB} uncertainty comes from the tracking efficiency.

In Fig. 5 we show a comparison of R_{FB} with the results of the theoretical calculations discussed above, except for the CGC-inspired model, which gives predictions only at forward rapidity. In addition, a prediction based on a LO approach, implementing a $2 \rightarrow 2$ kinematics ($gg \rightarrow J/\psi g$) and using either the EPS09 or the nDSG shadowing parameterization, is also shown [60]. The agreement between data and the model including both shadowing and coherent energy loss is very good, while pure shadowing scenarios seem to overestimate R_{FB} . However, it has to be noted that, although the experimental measurement of R_{FB} has a smaller uncertainty than R_{pPb} and R_{PbPb} , its comparison with theoretical calculations is less stringent, since models which globally overestimate/underestimate the nuclear modification factors may still provide a very good agreement with the measured R_{FB} .

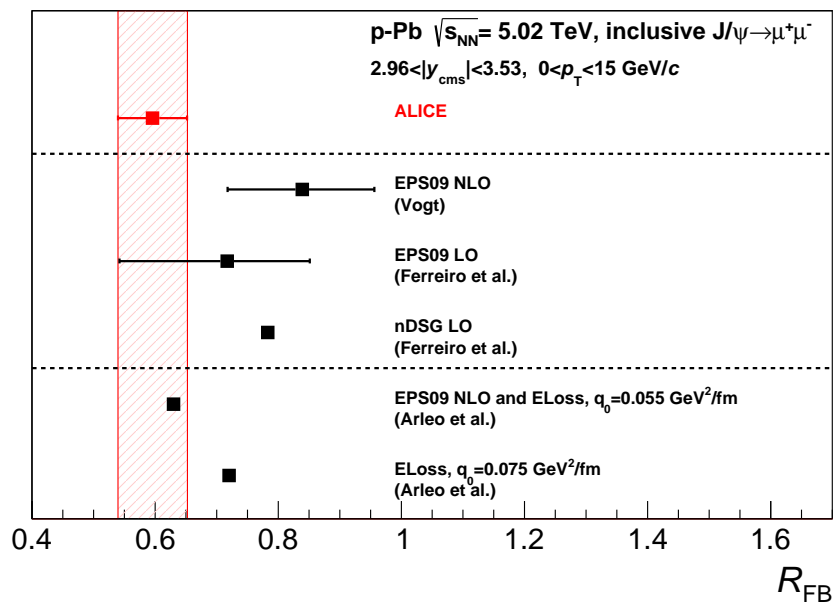


Fig. 5: The forward to backward ratio R_{FB} of the nuclear modification factors for inclusive J/ψ production, compared to theoretical models. The statistical and systematic uncertainties for the experimental value are added in quadrature. For the shadowing calculations, uncertainties are quoted when available, and are obtained in the same way as in Fig. 2.

The R_{FB} ratio has also been studied differentially in y (3 bins) and p_{T} (10 bins, covering the region $p_{\text{T}} < 15$ GeV/c). In Fig. 6 we show the results, again compared with the predictions of the models. The treatment of the uncertainties is the same described above for the integrated value of R_{FB} . As a function of rapidity, no variation is observed in the relatively narrow region covered by the R_{FB} measurement, while a trend towards higher R_{FB} values is seen as p_{T} increases. Models including coherent energy loss seem to qualitatively reproduce the data, in particular when shadowing effects are taken into account, although they predict a steeper behaviour at low p_{T} [61].

Finally, the results presented in this paper provide information on the magnitude of cold nuclear matter effects in Pb-Pb collisions. ALICE has published results for R_{PbPb} in the region $2.5 < y_{\text{cms}} < 4$ at $\sqrt{s_{\text{NN}}} = 2.76$ TeV [24, 25]. Although the p-Pb data discussed above refer to slightly different y_{cms} regions and to a larger center of mass energy, the Bjorken- x regions probed by the J/ψ production process in the Pb nuclei for p-Pb and Pb-Pb are shifted by $\sim 10\%$ only. Indeed, in the so-called $2 \rightarrow 1$ approach, where the production kinematics is $gg \rightarrow J/\psi$ [62], the x -values selected in Pb-Pb collisions are $2 \cdot 10^{-5} < x <$

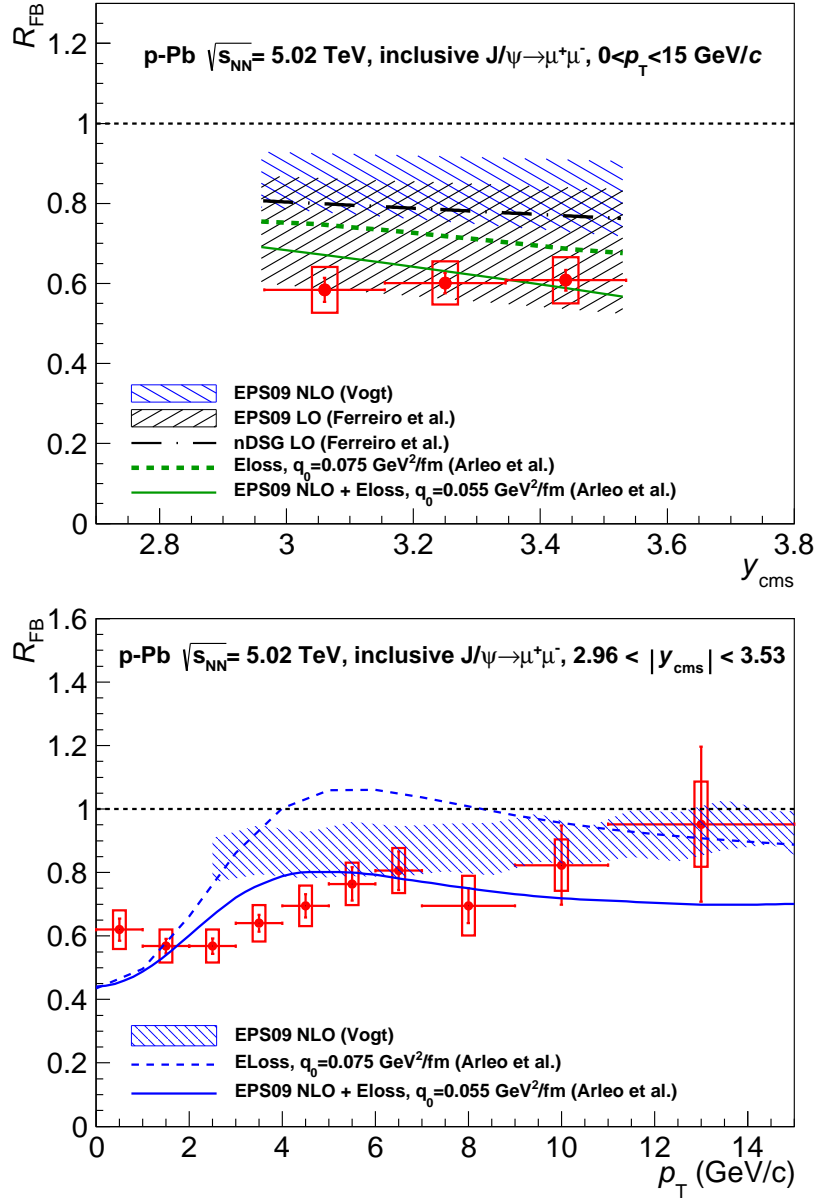


Fig. 6: The forward to backward ratio R_{FB} of the nuclear modification factors for inclusive J/ψ production, as a function of y and p_T , compared to theoretical models. The bars represent the statistical uncertainty, while the open boxes correspond to uncorrelated systematic uncertainties.

$9 \cdot 10^{-5}$, $1 \cdot 10^{-2} < x < 6 \cdot 10^{-2}$, the two ranges being relative to nucleons moving away from or toward the muon spectrometer, respectively. In proton-nucleus collisions, the probed x values for nucleons inside the Pb nucleus are $2 \cdot 10^{-5} < x < 8 \cdot 10^{-5}$ for p-Pb and $1 \cdot 10^{-2} < x < 5 \cdot 10^{-2}$ for Pb-p. If shadowing is the main nuclear effect, a hypothesis in fair agreement with the results shown in this paper, as a first approximation cold nuclear matter effects on R_{pPb} would be given by the product $R_{pPb} \times R_{PbP}$. This product is $0.75 \pm 0.10 \pm 0.12$ (the first uncertainty being related to the quadratical combination of statistical and uncorrelated systematic uncertainties, the second one coming from the linear combination of correlated uncertainties), which is larger than $R_{pPb} = 0.57 \pm 0.01 \pm 0.09$ [25]. This could be an indication that the J/ψ suppression effect observed in Pb-Pb collisions cannot be ascribed to cold nuclear matter effects alone. However, the size of the uncertainties prevents a strong conclusion on this point.

In summary, inclusive J/ψ production has been measured with the ALICE detector in p-Pb collisions at the CERN LHC. In this paper we have presented the production cross sections and the nuclear modification factors in the regions $2.03 < y_{cms} < 3.53$ and $-4.46 < y_{cms} < -2.96$, as well as their ratio R_{FB} in the region $2.96 < |y_{cms}| < 3.53$. While at forward rapidity (R_{pPb}) a suppression with respect to pp collisions is observed, in the backward region (R_{PbP}) no suppression is present. A fair agreement is seen with predictions based on a pure nuclear shadowing scenario [55, 60], parameterized using the EPS09 approach, as well as with models including a contribution from coherent partonic energy loss [13]. None of these models include a final state break-up of the J/ψ in cold nuclear matter. The study of R_{FB} , carried out as a function of y and p_T , confirms these indications. Finally, the results presented in this paper provide an important baseline for the interpretation of heavy-ion collision results and are in agreement with those presented by the LHCb Collaboration [63].

Acknowledgements

The ALICE collaboration is grateful for useful discussions with the LHCb collaboration. The ALICE collaboration would like to thank all its engineers and technicians for their invaluable contributions to the construction of the experiment and the CERN accelerator teams for the outstanding performance of the LHC complex. The ALICE collaboration acknowledges the following funding agencies for their support in building and running the ALICE detector: State Committee of Science, World Federation of Scientists (WFS) and Swiss Fonds Kidagan, Armenia, Conselho Nacional de Desenvolvimento Científico e Tecnológico (CNPq), Financiadora de Estudos e Projetos (FINEP), Fundação de Amparo à Pesquisa do Estado de São Paulo (FAPESP); National Natural Science Foundation of China (NSFC), the Chinese Ministry of Education (CMOE) and the Ministry of Science and Technology of China (MSTC); Ministry of Education and Youth of the Czech Republic; Danish Natural Science Research Council, the Carlsberg Foundation and the Danish National Research Foundation; The European Research Council under the European Community's Seventh Framework Programme; Helsinki Institute of Physics and the Academy of Finland; French CNRS-IN2P3, the 'Region Pays de Loire', 'Region Alsace', 'Region Auvergne' and CEA, France; German BMBF and the Helmholtz Association; General Secretariat for Research and Technology, Ministry of Development, Greece; Hungarian OTKA and National Office for Research and Technology (NKTH); Department of Atomic Energy and Department of Science and Technology of the Government of India; Istituto Nazionale di Fisica Nucleare (INFN) and Centro Fermi - Museo Storico della Fisica e Centro Studi e Ricerche "Enrico Fermi", Italy; MEXT Grant-in-Aid for Specially Promoted Research, Japan; Joint Institute for Nuclear Research, Dubna; National Research Foundation of Korea (NRF); CONACYT, DGAPA, México, ALFA-EC and the EPLANET Program (European Particle Physics Latin American Network) Stichting voor Fundamenteel Onderzoek der Materie (FOM) and the Nederlandse Organisatie voor Wetenschappelijk Onderzoek (NWO), Netherlands; Research Council of Norway (NFR); Polish Ministry of Science and Higher Education; National Authority for Scientific Research - NASR (Autoritatea Națională pentru Cercetare Științifică - ANCS); Ministry of Education and Science of Russian Federation, Russian Academy of Sciences, Russian Federal Agency of Atomic

Energy, Russian Federal Agency for Science and Innovations and The Russian Foundation for Basic Research; Ministry of Education of Slovakia; Department of Science and Technology, South Africa; CIEMAT, EELA, Ministerio de Economía y Competitividad (MINECO) of Spain, Xunta de Galicia (Consellería de Educación), CEADEN, Cubaenergía, Cuba, and IAEA (International Atomic Energy Agency); Swedish Research Council (VR) and Knut & Alice Wallenberg Foundation (KAW); Ukraine Ministry of Education and Science; United Kingdom Science and Technology Facilities Council (STFC); The United States Department of Energy, the United States National Science Foundation, the State of Texas, and the State of Ohio.

References

- [1] N. Brambilla et al., *Eur. Phys. J.* **C71**(2011) 1534.
- [2] G.T. Bodwin, E. Braaten and G.P. Lepage, *Phys. Rev.* **D51**(1995) 1125.
- [3] M. Butenschoen and B.A. Kniehl, *Phys. Rev. Lett.* **106**(2011) 022003.
- [4] J.J. Aubert et al. (EMC Collaboration), *Phys. Lett.* **B123**(1983) 275.
- [5] K.J. Eskola, H. Paukkunen and C.A. Salgado, *JHEP* **0904**(2009) 065.
- [6] D. de Florian, R. Sassot, P. Zurita and M. Stratmann, *Phys. Rev.* **D85**(2012) 0704028.
- [7] D. de Florian and R. Sassot, *Phys. Rev.* **D69**(2004) 0704028.
- [8] M. Hirai, S. Kumano and T. H. Nagai, *Phys. Rev.* **C76**(2007) 065207.
- [9] D. Kharzeev and K. Tuchin, *Nucl. Phys.* **A770**(2006) 40.
- [10] H. Fujii, F. Gelis and R. Venugopalan, *Nucl. Phys.* **A780**(2006) 146.
- [11] S. Gavin and J. Milana, *Phys. Rev. Lett.* **68**(1992) 1834.
- [12] S. Brodsky and P. Hoyer, *Phys. Lett.* **B298**(1993) 165.
- [13] F. Arleo and S. Peigné, *Phys. Rev. Lett.* **109**(2012) 122301.
- [14] R. Vogt, *Nucl. Phys.* **A700**(2002) 539.
- [15] B.Z. Kopeliovich and B.G. Zakharov, *Phys. Rev.* **D44**(2001) 3466.
- [16] D. McGlinchey, A.D. Frawley and R. Vogt, *Phys.Rev.* **C87**(2013) 054910.
- [17] R. Vogt, *Phys. Rev.* **C61**(2000) 035203.
- [18] T. Matsui and H. Satz, *Phys. Lett.* **B178**(1986) 416.
- [19] B. Alessandro et al. (NA50 Collaboration), *Eur. Phys. J.* **C39**(2005) 335.
- [20] R. Arnaldi et al. (NA60 Collaboration), *Phys. Rev. Lett.* **99**(2007) 132302.
- [21] R. Arnaldi et al. (NA60 Collaboration), *Nucl. Phys.* **A830**(2009) 345c.
- [22] A. Adare et al. (PHENIX Collaboration), *Phys. Rev.* **C84**(2011) 054912.
- [23] B.I. Abelev et al. (STAR Collaboration), *Phys. Rev.* **C80**(2009) 41902.
- [24] B. Abelev et al. (ALICE Collaboration), *Phys. Rev. Lett.* **109**(2012) 072301.
- [25] B. Abelev et al. (ALICE Collaboration), arXiv:1311.0214, submitted to *Phys. Lett. B*.
- [26] S. Chatrchyan et al. (CMS Collaboration), *JHEP* **1205**(2012) 063.
- [27] G. Aad et al. (ATLAS Collaboration), *Phys. Lett.* **B697**(2011) 294.
- [28] B. Alessandro et al. (NA50 Collaboration), *Phys. Lett.* **B553**(2003) 167.
- [29] A. Adare et al. (PHENIX Collaboration), *Phys. Rev. Lett.* **107**(2011) 142301.
- [30] B. Alessandro et al. (NA50 Collaboration), *Eur. Phys. J.* **C48**(2006) 329.
- [31] R. Arnaldi et al. (NA60 Collaboration), *Phys. Lett.* **B706**(2012) 263.
- [32] M.J. Leitch et al. (E866 Collaboration), *Phys. Rev. Lett.* **84**(2000) 3256.
- [33] I. Abt et al. (HERA-B Collaboration), *Eur. Phys. J.* **C 60**(2009) 525.
- [34] A. Adare et al. (PHENIX Collaboration), *Phys. Rev. C* **87**(2013) 034904.

- [35] K. Aamodt et al. (ALICE Collaboration), Phys. Lett. **B 704**(2011) 442.
- [36] K. Aamodt et al. (ALICE Collaboration), JINST **5**(2010) P03003.
- [37] E. Abbas et al. (ALICE Collaboration), JINST **8**(2013) P10016.
- [38] B. Abelev et al. (ALICE Collaboration), Phys. Rev. Lett. **109**(2012) 252302.
- [39] K. Aamodt et al. (ALICE Collaboration), JINST **3**(2008) S08002.
- [40] B. Abelev et al. (ALICE Collaboration), Phys. Rev. Lett. **110**(2013) 032301.
- [41] B. Abelev et al., “Measurement of visible cross-sections in proton-lead collisions at $\sqrt{s_{NN}}=5.02$ TeV in van der Meer scans with the ALICE detector”, in preparation.
- [42] J. Gaiser, SLAC Stanford - SLAC-255 (82.REC.JUN.83) 194p, <http://www.slac.stanford.edu/cgi-wrap/getdoc/slac-r-255.pdf>.
- [43] R. Shahoyan, Ph.D. Thesis, Instituto Superior Técnico, Lisbon, Portugal, 2001, <http://www.cern.ch/NA50/theses/ruben.ps.gz>.
- [44] J. Beringer et al. (Particle Data Group), Phys. Rev. **D86**(2012) 010001.
- [45] B. Abelev et al. (ALICE Collaboration), Phys. Rev. Lett. **108** (2012) 082001.
- [46] R. Aaij et al. (LHCb Collaboration), arXiv:1307.6379.
- [47] S. Chatrchyan et al. (CMS Collaboration), arXiv:1307.6070.
- [48] B. Abelev et al. (ALICE Collaboration), Phys. Rev. Lett. **110**(2013) 082302.
- [49] ALICE/LHCb joint public note, ALICE-PUBLIC-2013-002, LHCb-CONF-2013-013.
- [50] B. Abelev et al. (ALICE Collaboration), Phys. Lett. **B718**(2012) 295.
- [51] B. Abelev et al. (ALICE Collaboration), “Measurement of quarkonium production at forward rapidity in pp collisions at $\sqrt{s} = 7$ TeV with the ALICE detector”, in preparation.
- [52] M. Glück, J.F. Owens and E. Reya, Phys. Rev. **D17**(1978) 2324.
- [53] M. Cacciari, M. Greco and P. Nason, JHEP **9805**(1998) 007.
- [54] F. Bossù et al., arXiv:1103.2394.
- [55] R. Vogt, Int. J. Mod. Phys. **E22**(2013) 1330007 and priv. comm.
- [56] F. Arleo and S. Peigné, JHEP **1303**(2013) 122.
- [57] H. Fujii and K. Watanabe, Nucl. Phys. **A915**(2013) 1.
- [58] R. Aaij et al. (LHCb Collaboration), JHEP **1302**(2013) 041.
- [59] R. Aaij et al. (LHCb Collaboration), Eur. Phys. J. **C71**(2011) 1645.
- [60] E. Ferreira et al., arXiv:1305.4569.
- [61] F. Arleo, R. Kolevatov, S. Peigné and M. Rustamova, JHEP **1305**(2013) 155.
- [62] R. Vogt, Phys. Rev. **C71**(2005) 054902.
- [63] R. Aaij et al. (LHCb Collaboration), CERN-PH-EP-2013-156, LHCb-PAPER-2013-052, submitted to JHEP.

A The ALICE Collaboration

B. Abelev⁷⁰, J. Adam³⁶, D. Adamová⁷⁸, A.M. Adare¹²⁸, M.M. Aggarwal⁸², G. Aglieri Rinella³³, M. Agnello^{88,105}, A.G. Agocs¹²⁷, A. Agostinelli²⁵, Z. Ahammed¹²³, N. Ahmad¹⁶, A. Ahmad Masoodi¹⁶, I. Ahmed¹⁴, S.U. Ahn⁶³, S.A. Ahn⁶³, I. Aimo^{105,88}, S. Aiola¹²⁸, M. Ajaz¹⁴, A. Akindinov⁵⁴, D. Aleksandrov⁹⁴, B. Alessandro¹⁰⁵, D. Alexandre⁹⁶, A. Alici^{11,99}, A. Alkin³, J. Alme³⁴, T. Alt³⁸, V. Altini³⁰, S. Altinpinar¹⁷, I. Altsybeev¹²², C. Alves Garcia Prado¹¹², C. Andrei⁷³, A. Andronic⁹¹, V. Anguelov⁸⁷, J. Anielski⁴⁹, T. Antičić⁹², F. Antinori¹⁰², P. Antonioli⁹⁹, L. Aphecetche¹⁰⁶, H. Appelshäuser⁴⁷, N. Arbor⁶⁶, S. Arcelli²⁵, N. Armesto¹⁵, R. Arnaldi¹⁰⁵, T. Aronsson¹²⁸, I.C. Arsene⁹¹, M. Arslanok⁴⁷, A. Augustinus³³, R. Averbeck⁹¹, T.C. Awes⁷⁹, M.D. Azmi⁸⁴, M. Bach³⁸, A. Badalà¹⁰¹, Y.W. Baek^{39,65}, R. Bailhache⁴⁷, V. Bairathi⁸⁶, R. Bala⁸⁵, A. Baldisseri¹³, F. Baltasar Dos Santos Pedrosa³³, J. Bán⁵⁵, R.C. Baral⁵⁷, R. Barbera²⁶, F. Barile³⁰, G.G. Barnaföldi¹²⁷, L.S. Barnby⁹⁶, V. Barret⁶⁵, J. Bartke¹⁰⁹, M. Basile²⁵, N. Bastid⁶⁵, S. Basu¹²³, B. Bathen⁴⁹, G. Batigne¹⁰⁶, B. Batyunya⁶², P.C. Batzing²⁰, C. Baumann⁴⁷, I.G. Bearden⁷⁵, H. Beck⁴⁷, N.K. Behera⁴², I. Belikov⁵⁰, F. Bellini²⁵, R. Bellwied¹¹⁴, E. Belmont-Moreno⁶⁰, G. Bencedi²⁷, S. Beole²⁴, I. Berceau⁷³, A. Bercuci⁷³, Y. Berdnikov⁸⁰, D. Berenyi¹²⁷, A.A.E. Bergognon¹⁰⁶, R.A. Bertens⁵³, D. Berzano²⁴, L. Betev³³, A. Bhasin⁸⁵, A.K. Bhati⁸², J. Bhom¹¹⁹, L. Bianchi²⁴, N. Bianchi⁶⁷, C. Bianchin⁵³, J. Bielčik³⁶, J. Bielčíková⁷⁸, A. Bilandzic⁷⁵, S. Bjelogrić⁵³, F. Blanco⁹, D. Blau⁹⁴, C. Blume⁴⁷, F. Bock^{87,69}, A. Bogdanov⁷¹, H. Bøggild⁷⁵, M. Bogolyubsky⁵¹, L. Boldizsár¹²⁷, M. Bombara³⁷, J. Book⁴⁷, H. Borel¹³, A. Borissov^{126,90}, J. Bornschein³⁸, F. Bossú⁶¹, M. Botje⁷⁶, E. Botta²⁴, S. Böttger⁴⁶, P. Braun-Munzinger⁹¹, M. Bregant^{112,106}, T. Breitner⁴⁶, T.A. Broker⁴⁷, T.A. Browning⁸⁹, M. Broz³⁵, R. Brun³³, E. Bruna¹⁰⁵, G.E. Bruno³⁰, D. Budnikov⁹³, H. Buesching⁴⁷, S. Bufalino¹⁰⁵, P. Buncic³³, O. Busch⁸⁷, Z. Buthelezi⁶¹, D. Caffarri²⁷, X. Cai⁶, H. Caines¹²⁸, A. Caliva⁵³, E. Calvo Villar⁹⁷, P. Camerini²³, V. Canoa Roman^{10,33}, F. Carena³³, W. Carena³³, F. Carminati³³, A. Casanova Díaz⁶⁷, J. Castillo Castellanos¹³, E.A.R. Casula²², V. Catanesu⁷³, C. Cavicchioli³³, C. Ceballos Sanchez⁸, J. Cepila³⁶, P. Cerello¹⁰⁵, B. Chang¹¹⁵, S. Chapeland³³, J.L. Charvet¹³, S. Chattopadhyay⁹⁵, S. Chattopadhyay¹²³, M. Cherney⁸¹, C. Cheshkov¹²¹, B. Cheynis¹²¹, V. Chibante Barroso³³, D.D. Chinellato^{113,114}, P. Chochula³³, M. Chojnacki⁷⁵, S. Choudhury¹²³, P. Christakoglou⁷⁶, C.H. Christensen⁷⁵, P. Christiansen³¹, T. Chujo¹¹⁹, S.U. Chung⁹⁰, C. Cicalo¹⁰⁰, L. Cifarelli^{25,11}, F. Cindolo⁹⁹, J. Cleymans⁸⁴, F. Colamaria³⁰, D. Colella³⁰, A. Collu²², M. Colocci²⁵, G. Conesa Balbastre⁶⁶, Z. Conesa del Valle^{45,33}, M.E. Connors¹²⁸, G. Contin²³, J.G. Contreras¹⁰, T.M. Cormier¹²⁶, Y. Corrales Morales²⁴, P. Cortese²⁹, I. Cortés Maldonado², M.R. Cosentino^{112,69}, F. Costa³³, P. Crochet⁶⁵, R. Cruz Albino¹⁰, E. Cuaule⁵⁹, L. Cunqueiro^{33,67}, A. Dainese¹⁰², R. Dang⁶, A. Danu⁵⁸, K. Das⁹⁵, I. Das⁴⁵, D. Das⁹⁵, A. Dash¹¹³, S. Dash⁴², S. De¹²³, H. Delagrange¹⁰⁶, A. Deloff⁷², E. Dénes¹²⁷, A. Deppman¹¹², G. D'Erasmus³⁰, G.O.V. de Barros¹¹², A. De Caro^{28,11}, G. de Cataldo⁹⁸, J. de Cuveland³⁸, A. De Falco²², D. De Gruttola^{11,28}, N. De Marco¹⁰⁵, S. De Pasquale²⁸, R. de Rooij⁵³, M.A. Diaz Corchero⁹, T. Dietel^{49,84}, R. Divià³³, D. Di Bari³⁰, C. Di Giglio³⁰, S. Di Liberto¹⁰³, A. Di Mauro³³, P. Di Nezza⁶⁷, Ø. Djuvsland¹⁷, A. Dobrin^{53,126}, T. Dobrowolski⁷², D. Domenicis Gimenez¹¹², B. Dönigus^{91,47}, O. Dordic²⁰, A.K. Dubey¹²³, A. Dubla⁵³, L. Ducroux¹²¹, P. Dupieux⁶⁵, A.K. Dutta Majumdar⁹⁵, D. Elia⁹⁸, D. Emschermann⁴⁹, H. Engel⁴⁶, B. Erazmus^{33,106}, H.A. Erdal³⁴, D. Eschweiler³⁸, B. Espagnon⁴⁵, M. Estienne¹⁰⁶, S. Esumi¹¹⁹, D. Evans⁹⁶, S. Evdokimov⁵¹, G. Eyyubova²⁰, D. Fabris¹⁰², J. Faivre⁶⁶, D. Falchieri²⁵, A. Fantoni⁶⁷, M. Fasel⁸⁷, D. Fehler¹⁷, L. Feldkamp⁴⁹, D. Felea⁵⁸, A. Feliciello¹⁰⁵, G. Feofilov¹²², J. Ferencei⁷⁸, A. Fernández Téllez², E.G. Ferreira¹⁵, A. Ferretti²⁴, A. Festanti²⁷, J. Figiel¹⁰⁹, M.A.S. Figueredo^{112,116}, S. Filchagin⁹³, D. Finogeev⁵², F.M. Fionda³⁰, E.M. Fiore³⁰, E. Floratos⁸³, M. Floris³³, S. Foertsch⁶¹, P. Foka⁹¹, S. Fokin⁹⁴, E. Fragiaco¹⁰⁴, A. Francescon^{27,33}, U. Frankenfeld⁹¹, U. Fuchs³³, C. Furget⁶⁶, M. Fusco Girard²⁸, J.J. Gaardhøje⁷⁵, M. Gagliardi²⁴, M. Gallio²⁴, D.R. Gangadharan^{18,69}, P. Ganoti⁷⁹, C. Garabatos⁹¹, E. Garcia-Solis¹², C. Gargiulo³³, I. Garishvili⁷⁰, J. Gerhard³⁸, M. Germain¹⁰⁶, A. Gheata^{33,58}, B. Ghidini³⁰, P. Ghosh¹²³, P. Gianotti⁶⁷, P. Giubellino³³, E. Gladysz-Dziadus¹⁰⁹, P. Glässel⁸⁷, R. Gomez^{111,10}, P. González-Zamora⁹, S. Gorbunov³⁸, L. Görlich¹⁰⁹, S. Gotovac¹⁰⁸, L.K. Graczykowski¹²⁵, R. Grajcarek⁸⁷, A. Grelli⁵³, A. Grigoras³³, C. Grigoras³³, V. Grigoriev⁷¹, S. Grigoryan⁶², A. Grigoryan¹, B. Grinyov³, N. Grion¹⁰⁴, J.F. Grosse-Oetringhaus³³, J.-Y. Grossiord¹²¹, R. Grosso³³, F. Guber⁵², R. Guernane⁶⁶, B. Guerzoni²⁵, M. Guilbaud¹²¹, K. Gulbrandsen⁷⁵, H. Gulkanyan¹, T. Gunji¹¹⁸, A. Gupta⁸⁵, R. Gupta⁸⁵, K. H. Khan¹⁴, R. Haake⁴⁹, Ø. Haaland¹⁷, C. Hadjidakis⁴⁵, M. Haiduc⁵⁸, H. Hamagaki¹¹⁸, G. Hamar¹²⁷, L.D. Hanratty⁹⁶, A. Hansen⁷⁵, J.W. Harris¹²⁸, H. Hartmann³⁸, A. Harton¹², D. Hatzifotiadou⁹⁹, S. Hayashi¹¹⁸, A. Hayrapetyan^{33,1}, S.T. Heckel⁴⁷, M. Heide⁴⁹, H. Helstrup³⁴, A. Herghelegiu⁷³, G. Herrera Corral¹⁰, N. Herrmann⁸⁷, B.A. Hess³², K.F. Hetland³⁴, B. Hicks¹²⁸, B. Hippolyte⁵⁰, Y. Hori¹¹⁸, P. Hristov³³, I. Hřivnáčová⁴⁵, M. Huang¹⁷, T.J. Humanic¹⁸, D. Hutter³⁸, D.S. Hwang¹⁹, R. Ilkaev⁹³, I. Ilkiv⁷², M. Inaba¹¹⁹, E. Incani²², G.M. Innocenti²⁴, C. Ionita³³, M. Ippolitov⁹⁴, M. Irfan¹⁶, M. Ivanov⁹¹, V. Ivanov⁸⁰,

O. Ivanytskyi³, A. Jacholkowski²⁶, C. Jahnke¹¹², H.J. Jang⁶³, M.A. Janik¹²⁵, P.H.S.Y. Jayarathna¹¹⁴, S. Jena^{42, 114}, R.T. Jimenez Bustamante⁵⁹, P.G. Jones⁹⁶, H. Jung³⁹, A. Jusko⁹⁶, S. Kalcher³⁸, P. Kaliňák⁵⁵, A. Kalweit³³, J.H. Kang¹²⁹, V. Kaplin⁷¹, S. Kar¹²³, A. Karasu Uysal⁶⁴, O. Karavichev⁵², T. Karavicheva⁵², E. Karpechev⁵², U. Kebschull⁴⁶, R. Keidel¹³⁰, M. Mohisin. Khan^{16, ii}, S.A. Khan¹²³, P. Khan⁹⁵, A. Khanzadeev⁸⁰, Y. Kharlov⁵¹, B. Kileng³⁴, J.S. Kim³⁹, D.W. Kim^{63, 39}, D.J. Kim¹¹⁵, T. Kim¹²⁹, B. Kim¹²⁹, S. Kim¹⁹, M. Kim¹²⁹, M. Kim³⁹, S. Kirsch³⁸, I. Kisel³⁸, S. Kiselev⁵⁴, A. Kisiel¹²⁵, G. Kiss¹²⁷, J.L. Klay⁵, J. Klein⁸⁷, C. Klein-Bösing⁴⁹, A. Kluge³³, M.L. Knichel⁹¹, A.G. Knospe¹¹⁰, C. Kobdaj^{33, 107}, M.K. Köhler⁹¹, T. Kollegger³⁸, A. Kolojvari¹²², V. Kondratiev¹²², N. Kondratyeva⁷¹, A. Konevskikh⁵², V. Kovalenko¹²², M. Kowalski¹⁰⁹, S. Kox⁶⁶, G. Koyithatta Meethalevedu⁴², J. Kral¹¹⁵, I. Králik⁵⁵, F. Kramer⁴⁷, A. Kravčáková³⁷, M. Krelina³⁶, M. Kretz³⁸, M. Krivda^{55, 96}, F. Krizek^{78, 40, 36}, M. Krus³⁶, E. Kryshen⁸⁰, M. Krzewicki⁹¹, V. Kučera⁷⁸, Y. Kucheriaev⁹⁴, T. Kugathan³³, C. Kuhn⁵⁰, P.G. Kuijter⁷⁶, I. Kulakov⁴⁷, J. Kumar⁴², P. Kurashvili⁷², A.B. Kurepin⁵², A. Kurepin⁵², A. Kuryakin⁹³, V. Kushpil⁷⁸, S. Kushpil⁷⁸, M.J. Kweon^{44, 87}, Y. Kwon¹²⁹, P. Ladron de Guevara⁵⁹, C. Lagana Fernandes¹¹², I. Lakomov⁴⁵, R. Langoy¹²⁴, C. Lara⁴⁶, A. Lardeux¹⁰⁶, A. Lattuca²⁴, S.L. La Pointe^{53, 105}, P. La Rocca²⁶, R. Lea²³, M. Lechman³³, G.R. Lee⁹⁶, S.C. Lee³⁹, I. Legrand³³, J. Lehnert⁴⁷, R.C. Lemmon⁷⁷, M. Lenhardt⁹¹, V. Lenti⁹⁸, E. Leogrande⁵³, M. Leoncino²⁴, I. León Monzón¹¹¹, P. Lévai¹²⁷, S. Li^{6, 65}, J. Lien^{124, 17}, R. Lietava⁹⁶, S. Lindal²⁰, V. Lindenstruth³⁸, C. Lippmann⁹¹, M.A. Lisa¹⁸, H.M. Ljunggren³¹, D.F. Lodato⁵³, P.I. Loenne¹⁷, V.R. Loggins¹²⁶, V. Loginov⁷¹, D. Lohner⁸⁷, C. Loizides⁶⁹, X. Lopez⁶⁵, E. López Torres⁸, X.-G. Lu⁸⁷, P. Luetig⁴⁷, M. Lunardon²⁷, J. Luo⁶, G. Luparello⁵³, C. Luzzi³³, A. M. Gago⁹⁷, P. M. Jacobs⁶⁹, R. Ma¹²⁸, A. Maevskaya⁵², M. Mager³³, D.P. Mahapatra⁵⁷, A. Maire⁸⁷, M. Malaev⁸⁰, I. Maldonado Cervantes⁵⁹, L. Malinina^{62, iii}, D. Mal'Kevich⁵⁴, P. Malzacher⁹¹, A. Mamonov⁹³, L. Manceau¹⁰⁵, V. Manko⁹⁴, F. Manso⁶⁵, V. Manzari^{98, 33}, M. Marchisone^{24, 65}, J. Mareš⁵⁶, G.V. Margagliotti²³, A. Margotti⁹⁹, A. Marín⁹¹, C. Markert^{110, 33}, M. Marquard⁴⁷, I. Martashvili¹¹⁷, N.A. Martin⁹¹, P. Martinengo³³, M.I. Martínez², G. Martínez García¹⁰⁶, J. Martin Blanco¹⁰⁶, Y. Martynov³, A. Mas¹⁰⁶, S. Masciocchi⁹¹, M. Maserà²⁴, A. Masoni¹⁰⁰, L. Massacrier¹⁰⁶, A. Mastroserio³⁰, A. Matyja¹⁰⁹, J. Mazer¹¹⁷, R. Mazumder⁴³, M.A. Mazzoni¹⁰³, F. Meddi²¹, A. Menchaca-Rocha⁶⁰, J. Mercado Pérez⁸⁷, M. Meres³⁵, Y. Miake¹¹⁹, K. Mikhaylov^{62, 54}, L. Milano³³, J. Milosevic^{20, iv}, A. Mischke⁵³, A.N. Mishra⁴³, D. Miśkowiec⁹¹, C.M. Mitu⁵⁸, J. Mlynar¹²⁶, B. Mohanty^{123, 74}, L. Molnar⁵⁰, L. Montaña Zetina¹⁰, E. Montes⁹, M. Morando²⁷, D.A. Moreira De Godoy¹¹², S. Moretto²⁷, A. Morreale¹¹⁵, A. Morsch³³, V. Muccifora⁶⁷, E. Mudnic¹⁰⁸, S. Muhuri¹²³, M. Mukherjee¹²³, H. Müller³³, M.G. Munhoz¹¹², S. Murray^{84, 61}, L. Musa³³, B.K. Nandi⁴², R. Nania⁹⁹, E. Nappi⁹⁸, C. Nattrass¹¹⁷, T.K. Nayak¹²³, S. Nazarenko⁹³, A. Nedosekin⁵⁴, M. Nicassio^{30, 91}, M. Niculescu^{33, 58}, B.S. Nielsen⁷⁵, S. Nikolaev⁹⁴, S. Nikulin⁹⁴, V. Nikulin⁸⁰, B.S. Nilsen⁸¹, F. Noferini^{11, 99}, P. Nomokonov⁶², G. Nooren⁵³, A. Nyman⁹⁴, A. Nyatha⁴², J. Nystrand¹⁷, H. Oeschler^{87, 48}, S.K. Oh^{39, v}, S. Oh¹²⁸, L. Olah¹²⁷, J. Oleniacz¹²⁵, A.C. Oliveira Da Silva¹¹², J. Onderwaater⁹¹, C. Oppedisano¹⁰⁵, A. Ortiz Velasquez³¹, A. Oskarsson³¹, J. Otwinowski⁹¹, K. Oyama⁸⁷, Y. Pachmayer⁸⁷, M. Pachr³⁶, P. Pagano²⁸, G. Paic⁵⁹, F. Painke³⁸, C. Pajares¹⁵, S.K. Pal¹²³, A. Palaha⁹⁶, A. Palmeri¹⁰¹, V. Papikyan¹, G.S. Pappalardo¹⁰¹, W.J. Park⁹¹, A. Passfeld⁴⁹, D.I. Patalakha⁵¹, V. Paticchio⁹⁸, B. Paul⁹⁵, T. Pawlak¹²⁵, T. Peitzmann⁵³, H. Pereira Da Costa¹³, E. Pereira De Oliveira Filho¹¹², D. Peresunko⁹⁴, C.E. Pérez Lara⁷⁶, D. Perrino³⁰, W. Peryt^{125, i}, A. Pesci⁹⁹, Y. Pestov⁴, V. Petráček³⁶, M. Petran³⁶, M. Petris⁷³, P. Petrov⁹⁶, M. Petrovici⁷³, C. Petta²⁶, S. Piano¹⁰⁴, M. Pikna³⁵, P. Pillot¹⁰⁶, O. Pinazza^{33, 99}, L. Pinsky¹¹⁴, N. Pitz⁴⁷, D.B. Piyarathna¹¹⁴, M. Planinic^{92, 120}, M. Płoskoń⁶⁹, J. Pluta¹²⁵, S. Pochybova¹²⁷, P.L.M. Podesta-Lerma¹¹¹, M.G. Poghosyan³³, E.H.O. Pohjoisaho⁴⁰, B. Polichtchouk⁵¹, A. Pop⁷³, S. Porteboeuf-Houssais⁶⁵, V. Pospíšil³⁶, B. Potukuchi⁸⁵, S.K. Prasad¹²⁶, R. Preghenella^{11, 99}, F. Prino¹⁰⁵, C.A. Pruneau¹²⁶, I. Pshenichnov⁵², G. Puddu²², P. Pujahari^{42, 126}, V. Punin⁹³, J. Putschke¹²⁶, H. Qvigstad²⁰, A. Rachevski¹⁰⁴, A. Rademakers³³, J. Rak¹¹⁵, A. Rakotozafindrabe¹³, L. Ramello²⁹, S. Raniwala⁸⁶, R. Raniwala⁸⁶, S.S. Räsänen⁴⁰, B.T. Rascanu⁴⁷, D. Rathee⁸², W. Rauch³³, A.W. Rauf¹⁴, V. Razazi²², K.F. Read¹¹⁷, J.S. Real⁶⁶, K. Redlich^{72, vi}, R.J. Reed¹²⁸, A. Rehman¹⁷, P. Reichelt⁴⁷, M. Reicher⁵³, F. Reidt^{33, 87}, R. Renfordt⁴⁷, A.R. Reolon⁶⁷, A. Reshetin⁵², F. Rettig³⁸, J.-P. Revol³³, K. Reygers⁸⁷, L. Riccati¹⁰⁵, R.A. Ricci⁶⁸, T. Richert³¹, M. Richter²⁰, P. Riedler³³, W. Riegler³³, F. Riggi²⁶, A. Rivetti¹⁰⁵, M. Rodríguez Cahuantzi², A. Rodríguez Manso⁷⁶, K. Røed^{17, 20}, E. Rogochaya⁶², S. Rohni⁸⁵, D. Rohr³⁸, D. Röhrich¹⁷, F. Ronchetti⁶⁷, P. Rosnet⁶⁵, S. Rossegger³³, A. Rossi³³, P. Roy⁹⁵, C. Roy⁵⁰, A.J. Rubio Montero⁹, R. Rui²³, R. Russo²⁴, E. Ryabinkin⁹⁴, A. Rybicki¹⁰⁹, S. Sadovsky⁵¹, K. Šafařík³³, R. Sahoo⁴³, P.K. Sahu⁵⁷, J. Saini¹²³, H. Sakaguchi⁴¹, S. Sakai^{69, 67}, D. Sakata¹¹⁹, C.A. Salgado¹⁵, J. Salzwedel¹⁸, S. Sambyal⁸⁵, V. Samsonov⁸⁰, X. Sanchez Castro^{59, 50}, L. Šándor⁵⁵, A. Sandoval⁶⁰, M. Sano¹¹⁹, G. Santagati²⁶, R. Santoro^{11, 33}, D. Sarkar¹²³, E. Scapparone⁹⁹, F. Scarlassara²⁷, R.P. Scharenberg⁸⁹, C. Schiaua⁷³, R. Schicker⁸⁷, C. Schmidt⁹¹, H.R. Schmidt³², S. Schuchmann⁴⁷, J. Schukraft³³, M. Schulc³⁶, T. Schuster¹²⁸, Y. Schutz^{33, 106},

K. Schwarz⁹¹, K. Schweda⁹¹, G. Scioli²⁵, E. Scomparin¹⁰⁵, R. Scott¹¹⁷, P.A. Scott⁹⁶, G. Segato²⁷, I. Selyuzhenkov⁹¹, J. Seo⁹⁰, S. Serici²², E. Serradilla^{9,60}, A. Sevcenco⁵⁸, A. Shabetal¹⁰⁶, G. Shabratova⁶², R. Shahoyan³³, S. Sharma⁸⁵, N. Sharma¹¹⁷, K. Shigaki⁴¹, K. Shtejer²⁴, Y. Sibiraki⁹⁴, S. Siddhanta¹⁰⁰, T. Siemiarczuk⁷², D. Silvermyr⁷⁹, C. Silvestre⁶⁶, G. Simatovic¹²⁰, R. Singaraju¹²³, R. Singh⁸⁵, S. Singha^{74,123}, V. Singhal¹²³, T. Sinha⁹⁵, B.C. Sinha¹²³, B. Sitar³⁵, M. Sitta²⁹, T.B. Skaali²⁰, K. Skjerdal¹⁷, R. Smakal³⁶, N. Smirnov¹²⁸, R.J.M. Snellings⁵³, R. Soltz⁷⁰, M. Song¹²⁹, J. Song⁹⁰, C. Soos³³, F. Soramel²⁷, M. Spacek³⁶, I. Sputowska¹⁰⁹, M. Spyropoulou-Stassinaki⁸³, B.K. Srivastava⁸⁹, J. Stachel⁸⁷, I. Stan⁵⁸, G. Stefanek⁷², M. Steinpreis¹⁸, E. Stenlund³¹, G. Steyn⁶¹, J.H. Stiller⁸⁷, D. Stocco¹⁰⁶, M. Stolpovskiy⁵¹, P. Strmen³⁵, A.A.P. Suaide¹¹², M.A. Subieta Vasquez²⁴, T. Sugitate⁴¹, C. Suire⁴⁵, M. Suleymanov¹⁴, R. Sultanov⁵⁴, M. Šumbera⁷⁸, T. Susa⁹², T.J.M. Symons⁶⁹, A. Szanto de Toledo¹¹², I. Szarka³⁵, A. Szczepankiewicz³³, M. Szymanski¹²⁵, J. Takahashi¹¹³, M.A. Tangaro³⁰, J.D. Tapia Takaki⁴⁵, A. Tarantola Peloni⁴⁷, A. Tarazona Martinez³³, A. Tauro³³, G. Tejeda Muñoz², A. Telesca³³, C. Terrevoli³⁰, A. Ter Minasyan^{94,71}, J. Thäder⁹¹, D. Thomas⁵³, R. Tieulent¹²¹, A.R. Timmins¹¹⁴, A. Toia¹⁰², H. Torii¹¹⁸, V. Trubnikov³, W.H. Trzaska¹¹⁵, T. Tsuji¹¹⁸, A. Tumkin⁹³, R. Turrisi¹⁰², T.S. Tvetter²⁰, J. Ulery⁴⁷, K. Ullaland¹⁷, J. Ulrich⁴⁶, A. Uras¹²¹, G.M. Urciuoli¹⁰³, G.L. Usai²², M. Vajzer⁷⁸, M. Vala^{55,62}, L. Valencia Palomo⁴⁵, P. Vande Vyvre³³, L. Vannucci⁶⁸, J.W. Van Hoorne³³, M. van Leeuwen⁵³, A. Vargas², R. Varma⁴², M. Vasileiou⁸³, A. Vasiliev⁹⁴, V. Vechernin¹²², M. Veldhoen⁵³, M. Venaruzzo²³, E. Vercellin²⁴, S. Vergara², R. Vernet⁷, M. Verweij^{126,53}, L. Vickovic¹⁰⁸, G. Viesti²⁷, J. Viinikainen¹¹⁵, Z. Vilakazi⁶¹, O. Villalobos Baillie⁹⁶, A. Vinogradov⁹⁴, L. Vinogradov¹²², Y. Vinogradov⁹³, T. Virgili²⁸, Y.P. Viyogi¹²³, A. Vodopyanov⁶², M.A. Völkl⁸⁷, K. Voloshin⁵⁴, S.A. Voloshin¹²⁶, G. Volpe³³, B. von Haller³³, I. Vorobyev¹²², D. Vranic^{33,91}, J. Vrláková³⁷, B. Vulpescu⁶⁵, A. Vyushin⁹³, B. Wagner¹⁷, V. Wagner³⁶, J. Wagner⁹¹, Y. Wang⁸⁷, Y. Wang⁶, M. Wang^{6,106}, D. Watanabe¹¹⁹, K. Watanabe¹¹⁹, M. Weber¹¹⁴, J.P. Wessels⁴⁹, U. Westerhoff⁴⁹, J. Wiechula³², J. Wikne²⁰, M. Wilde⁴⁹, G. Wilk⁷², J. Wilkinson⁸⁷, M.C.S. Williams⁹⁹, B. Windelband⁸⁷, M. Winn⁸⁷, C. Xiang⁶, C.G. Yaldo¹²⁶, Y. Yamaguchi¹¹⁸, H. Yang^{13,53}, P. Yang⁶, S. Yang¹⁷, S. Yano⁴¹, S. Yasnopolskiy⁹⁴, J. Yi⁹⁰, Z. Yin⁶, I.-K. Yoo⁹⁰, I. Yushmanov⁹⁴, V. Zaccolo⁷⁵, C. Zach³⁶, C. Zampolli⁹⁹, S. Zaporozhets⁶², A. Zarochentsev¹²², P. Závada⁵⁶, N. Zaviyalov⁹³, H. Zbroszczyk¹²⁵, P. Zelnicek⁴⁶, I.S. Zgura⁵⁸, M. Zhalov⁸⁰, Y. Zhang⁶, X. Zhang⁶, F. Zhang⁶, H. Zhang⁶, X. Zhang^{65,69}, C. Zhao²⁰, D. Zhou⁶, F. Zhou⁶, Y. Zhou⁵³, J. Zhu⁶, H. Zhu⁶, J. Zhu⁶, X. Zhu⁶, A. Zichichi^{25,11}, M.B. Zimmermann^{33,49}, A. Zimmermann⁸⁷, G. Zinovjev³, Y. Zoccarato¹²¹, M. Zynovyev³, M. Zyzak⁴⁷

Affiliation notes

- ⁱ Deceased
- ⁱⁱ Also at: Department of Applied Physics, Aligarh Muslim University, Aligarh, India
- ⁱⁱⁱ Also at: M.V.Lomonosov Moscow State University, D.V.Skobeltzyn Institute of Nuclear Physics, Moscow, Russia
- ^{iv} Also at: University of Belgrade, Faculty of Physics and "Vinča" Institute of Nuclear Sciences, Belgrade, Serbia
- ^v Permanent address: Konkuk University, Seoul, Korea
- ^{vi} Also at: Institute of Theoretical Physics, University of Wrocław, Wrocław, Poland

Collaboration Institutes

- ¹ A. I. Alikhanyan National Science Laboratory (Yerevan Physics Institute) Foundation, Yerevan, Armenia
- ² Benemérita Universidad Autónoma de Puebla, Puebla, Mexico
- ³ Bogolyubov Institute for Theoretical Physics, Kiev, Ukraine
- ⁴ Budker Institute for Nuclear Physics, Novosibirsk, Russia
- ⁵ California Polytechnic State University, San Luis Obispo, California, USA
- ⁶ Central China Normal University, Wuhan, China
- ⁷ Centre de Calcul de l
- ⁸ Centro de Aplicaciones Tecnológicas y Desarrollo Nuclear (CEADEN), Havana, Cuba
- ⁹ Centro de Investigaciones Energéticas Medioambientales y Tecnológicas (CIEMAT), Madrid, Spain
- ¹⁰ Centro de Investigación y de Estudios Avanzados (CINVESTAV), Mexico City and Mérida, Mexico
- ¹¹ Centro Fermi - Museo Storico della Fisica e Centro Studi e Ricerche "Enrico Fermi", Rome, Italy
- ¹² Chicago State University, Chicago, USA
- ¹³ Commissariat à l'Energie Atomique, IRFU, Saclay, France
- ¹⁴ COMSATS Institute of Information Technology (CIIT), Islamabad, Pakistan

- 15 Departamento de Física de Partículas and IGFAE, Universidad de Santiago de Compostela, Santiago de Compostela, Spain
- 16 Department of Physics Aligarh Muslim University, Aligarh, India
- 17 Department of Physics and Technology, University of Bergen, Bergen, Norway
- 18 Department of Physics, Ohio State University, Columbus, Ohio, USA
- 19 Department of Physics, Sejong University, Seoul, South Korea
- 20 Department of Physics, University of Oslo, Oslo, Norway
- 21 Dipartimento di Fisica dell
- 22 Dipartimento di Fisica dell'Università and Sezione INFN, Cagliari, Italy
- 23 Dipartimento di Fisica dell'Università and Sezione INFN, Trieste, Italy
- 24 Dipartimento di Fisica dell'Università and Sezione INFN, Turin, Italy
- 25 Dipartimento di Fisica e Astronomia dell'Università and Sezione INFN, Bologna, Italy
- 26 Dipartimento di Fisica e Astronomia dell'Università and Sezione INFN, Catania, Italy
- 27 Dipartimento di Fisica e Astronomia dell'Università and Sezione INFN, Padova, Italy
- 28 Dipartimento di Fisica 'E.R. Caianiello' dell'Università and Gruppo Collegato INFN, Salerno, Italy
- 29 Dipartimento di Scienze e Innovazione Tecnologica dell'Università del Piemonte Orientale and Gruppo Collegato INFN, Alessandria, Italy
- 30 Dipartimento Interateneo di Fisica 'M. Merlin' and Sezione INFN, Bari, Italy
- 31 Division of Experimental High Energy Physics, University of Lund, Lund, Sweden
- 32 Eberhard Karls Universität Tübingen, Tübingen, Germany
- 33 European Organization for Nuclear Research (CERN), Geneva, Switzerland
- 34 Faculty of Engineering, Bergen University College, Bergen, Norway
- 35 Faculty of Mathematics, Physics and Informatics, Comenius University, Bratislava, Slovakia
- 36 Faculty of Nuclear Sciences and Physical Engineering, Czech Technical University in Prague, Prague, Czech Republic
- 37 Faculty of Science, P.J. Šafárik University, Košice, Slovakia
- 38 Frankfurt Institute for Advanced Studies, Johann Wolfgang Goethe-Universität Frankfurt, Frankfurt, Germany
- 39 Gangneung-Wonju National University, Gangneung, South Korea
- 40 Helsinki Institute of Physics (HIP), Helsinki, Finland
- 41 Hiroshima University, Hiroshima, Japan
- 42 Indian Institute of Technology Bombay (IIT), Mumbai, India
- 43 Indian Institute of Technology Indore, India (IITI)
- 44 Inha University, College of Natural Sciences
- 45 Institut de Physique Nucleaire d'Orsay (IPNO), Universite Paris-Sud, CNRS-IN2P3, Orsay, France
- 46 Institut für Informatik, Johann Wolfgang Goethe-Universität Frankfurt, Frankfurt, Germany
- 47 Institut für Kernphysik, Johann Wolfgang Goethe-Universität Frankfurt, Frankfurt, Germany
- 48 Institut für Kernphysik, Technische Universität Darmstadt, Darmstadt, Germany
- 49 Institut für Kernphysik, Westfälische Wilhelms-Universität Münster, Münster, Germany
- 50 Institut Pluridisciplinaire Hubert Curien (IPHC), Université de Strasbourg, CNRS-IN2P3, Strasbourg, France
- 51 Institute for High Energy Physics, Protvino, Russia
- 52 Institute for Nuclear Research, Academy of Sciences, Moscow, Russia
- 53 Institute for Subatomic Physics of Utrecht University, Utrecht, Netherlands
- 54 Institute for Theoretical and Experimental Physics, Moscow, Russia
- 55 Institute of Experimental Physics, Slovak Academy of Sciences, Košice, Slovakia
- 56 Institute of Physics, Academy of Sciences of the Czech Republic, Prague, Czech Republic
- 57 Institute of Physics, Bhubaneswar, India
- 58 Institute of Space Science (ISS), Bucharest, Romania
- 59 Instituto de Ciencias Nucleares, Universidad Nacional Autónoma de México, Mexico City, Mexico
- 60 Instituto de Física, Universidad Nacional Autónoma de México, Mexico City, Mexico
- 61 iThemba LABS, National Research Foundation, Somerset West, South Africa
- 62 Joint Institute for Nuclear Research (JINR), Dubna, Russia
- 63 Korea Institute of Science and Technology Information, Daejeon, South Korea
- 64 KTO Karatay University, Konya, Turkey
- 65 Laboratoire de Physique Corpusculaire (LPC), Clermont Université, Université Blaise Pascal,

- CNRS-IN2P3, Clermont-Ferrand, France
- 66 Laboratoire de Physique Subatomique et de Cosmologie (LPSC), Université Joseph Fourier, CNRS-IN2P3, Institut Polytechnique de Grenoble, Grenoble, France
- 67 Laboratori Nazionali di Frascati, INFN, Frascati, Italy
- 68 Laboratori Nazionali di Legnaro, INFN, Legnaro, Italy
- 69 Lawrence Berkeley National Laboratory, Berkeley, California, USA
- 70 Lawrence Livermore National Laboratory, Livermore, California, USA
- 71 Moscow Engineering Physics Institute, Moscow, Russia
- 72 National Centre for Nuclear Studies, Warsaw, Poland
- 73 National Institute for Physics and Nuclear Engineering, Bucharest, Romania
- 74 National Institute of Science Education and Research, Bhubaneswar, India
- 75 Niels Bohr Institute, University of Copenhagen, Copenhagen, Denmark
- 76 Nikhef, National Institute for Subatomic Physics, Amsterdam, Netherlands
- 77 Nuclear Physics Group, STFC Daresbury Laboratory, Daresbury, United Kingdom
- 78 Nuclear Physics Institute, Academy of Sciences of the Czech Republic, Řež u Prahy, Czech Republic
- 79 Oak Ridge National Laboratory, Oak Ridge, Tennessee, USA
- 80 Petersburg Nuclear Physics Institute, Gatchina, Russia
- 81 Physics Department, Creighton University, Omaha, Nebraska, USA
- 82 Physics Department, Panjab University, Chandigarh, India
- 83 Physics Department, University of Athens, Athens, Greece
- 84 Physics Department, University of Cape Town, Cape Town, South Africa
- 85 Physics Department, University of Jammu, Jammu, India
- 86 Physics Department, University of Rajasthan, Jaipur, India
- 87 Physikalisches Institut, Ruprecht-Karls-Universität Heidelberg, Heidelberg, Germany
- 88 Politecnico di Torino, Turin, Italy
- 89 Purdue University, West Lafayette, Indiana, USA
- 90 Pusan National University, Pusan, South Korea
- 91 Research Division and ExtreMe Matter Institute EMMI, GSI Helmholtzzentrum für Schwerionenforschung, Darmstadt, Germany
- 92 Rudjer Bošković Institute, Zagreb, Croatia
- 93 Russian Federal Nuclear Center (VNIIEF), Sarov, Russia
- 94 Russian Research Centre Kurchatov Institute, Moscow, Russia
- 95 Saha Institute of Nuclear Physics, Kolkata, India
- 96 School of Physics and Astronomy, University of Birmingham, Birmingham, United Kingdom
- 97 Sección Física, Departamento de Ciencias, Pontificia Universidad Católica del Perú, Lima, Peru
- 98 Sezione INFN, Bari, Italy
- 99 Sezione INFN, Bologna, Italy
- 100 Sezione INFN, Cagliari, Italy
- 101 Sezione INFN, Catania, Italy
- 102 Sezione INFN, Padova, Italy
- 103 Sezione INFN, Rome, Italy
- 104 Sezione INFN, Trieste, Italy
- 105 Sezione INFN, Turin, Italy
- 106 SUBATECH, Ecole des Mines de Nantes, Université de Nantes, CNRS-IN2P3, Nantes, France
- 107 Suranaree University of Technology, Nakhon Ratchasima, Thailand
- 108 Technical University of Split FESB, Split, Croatia
- 109 The Henryk Niewodniczanski Institute of Nuclear Physics, Polish Academy of Sciences, Cracow, Poland
- 110 The University of Texas at Austin, Physics Department, Austin, TX, USA
- 111 Universidad Autónoma de Sinaloa, Culiacán, Mexico
- 112 Universidade de São Paulo (USP), São Paulo, Brazil
- 113 Universidade Estadual de Campinas (UNICAMP), Campinas, Brazil
- 114 University of Houston, Houston, Texas, USA
- 115 University of Jyväskylä, Jyväskylä, Finland
- 116 University of Liverpool, Liverpool, United Kingdom
- 117 University of Tennessee, Knoxville, Tennessee, USA
- 118 University of Tokyo, Tokyo, Japan

- ¹¹⁹ University of Tsukuba, Tsukuba, Japan
- ¹²⁰ University of Zagreb, Zagreb, Croatia
- ¹²¹ Université de Lyon, Université Lyon 1, CNRS/IN2P3, IPN-Lyon, Villeurbanne, France
- ¹²² V. Fock Institute for Physics, St. Petersburg State University, St. Petersburg, Russia
- ¹²³ Variable Energy Cyclotron Centre, Kolkata, India
- ¹²⁴ Vestfold University College, Tonsberg, Norway
- ¹²⁵ Warsaw University of Technology, Warsaw, Poland
- ¹²⁶ Wayne State University, Detroit, Michigan, USA
- ¹²⁷ Wigner Research Centre for Physics, Hungarian Academy of Sciences, Budapest, Hungary
- ¹²⁸ Yale University, New Haven, Connecticut, USA
- ¹²⁹ Yonsei University, Seoul, South Korea
- ¹³⁰ Zentrum für Technologietransfer und Telekommunikation (ZTT), Fachhochschule Worms, Worms, Germany